ISSN (Online) 2456 -1304

International Journal of Science, Engineering and Management (IJSEM)
Vol 3, Issue 3, March 2018

Adsorption of Acid Red 97 by A-Fe2o3 Nanopowder: Isotherm and Kinetic Studies

[1] Zulfiqar Ahmed M.N, [2] Chandrasekhar K.B, [3] Nagabhushana B.M
[1] Research Scholar, Jawaharlal Nehru Technological University Anantapur, Ananthapuramu, Andhra Pradesh, India
[2] Department of Chemistry, Jawaharlal Nehru Technological University Anantapur, Ananthapuramu, Andhra Pradesh, India
[3] Department of Chemistry, M.S Ramaiah Institute of Technology, MSR Nagar, Bangalore, Karnataka, India

Abstract: **-- α-Fe2O3 nanopowder was prepared by solution combustion synthesis using ferric nitrate as oxidiser and oxalyldihydrazide (ODH) as fuel. The characterization of the nanopowder was done by powder X-ray diffraction (PXRD), Fourier transform infrared spectroscopy (FTIR) and scanning electron microscopy (SEM). The potential of the nanopowder in the adsorption of Acid Red 97 dye was carried out at room temperature. The effect of parameters such as the adsorbent dosage, contact time and initial dye concentration was studied. Isotherm and kinetic studies were employed to analyze the adsorption data. The nanopowder was effective in removal of 20 ppm dye solution. The adsorption efficiency decreased as the initial concentration of the dye solution increased. The adsorption followed pseudo-first order kinetics and obeyed Dubinin-Radushkevich and Temkin adsorption isotherms.**

Index Terms— Solution Combustion Synthesis, α-Fe2O3 Nanopowder, Acid Red 97, Adsorption Isotherms, Adsorption Kinetics..

I. INTRODUCTION

Azo dyes are synthetic, coloured, organic compounds characterized by the presence of one or more azo groups (−N═O). Large amount of these dyes are synthesized worldwide and are used in various fields. However, about 15% of this total world production is usually lost during synthesis and processing steps. Hence, azo dyes are present in appreciable amounts in wastewater released from textile mills and dyestuff industries. The presence of these azo dyes in the wastewater poses a major threat to the surrounding ecosystems due to their non-biodegradable nature, toxicity and carcinogenic nature [1-3]. Various techniques available for dyes from wastewater include biological treatment, electroflocculation, filtration, adsorption, photocatalytic degradation etc. Among these techniques adsorption has attracted the attention of a large number of researchers across the globe. Activated carbon is the most widely used adsorbent material. However, its use is limited because of its expensive nature and also the requirement of additional effluent which adds up to the operational costs. Hence, the development of less expensive adsorbent materials for the removal of dyes and other pollutants from water is one of the major challenges faced by environmental engineering. Several low cost materials have been used by researchers for this purpose. Some of these materials include rice husk, clay, barks of trees, orange peel, apple pomace, wood, fly ash etc. In order, to get the adsorbent of required porosity and surface area, proper processing procedure has to be adopted which is the main drawback of these low cost adsorbents[4-7]. α-Fe2O3 nanoparticles exhibit unique properties such as superparamagnetism, high saturation fields and extra anisotropy contributions. These properties are the result of their finite size and large surface area. These properties make them useful materials in areas such as catalysis, magnetism, electrochemistry, biotechnology etc. [8-12].

Various methods have been employed by researchers for the preparation of α-Fe2O3 nanopowder. These methods include electrochemical anodization, surfactant-assisted solution method, hydrothermal method, sol-gel and solid state reaction method. Most of these methods suffer from various drawbacks such as long reaction times, requirement of high temperature etc. [13]. Solution combustion synthesis is an important method for the preparation of high purity nanomaterials such as oxides, silicates, chromates etc. in a short period of time. Further, the nanopowders possess high degree of crystallinity[14]. In the present study, α-Fe2O3 nanopowder was prepared by solution combustion synthesis and characterized by powder X-ray diffraction (PXRD), Fourier transform infrared spectroscopy (FTIR) and scanning electron microscopy (SEM). The potential of the nanopowder as an adsorbent for the removal of the dye Acid Red 97 (AR 97) from its aqueous solution was studied. The effect of parameters such as adsorbent dosage, contact time

ISSN (Online) 2456 -1304

International Journal of Science, Engineering and Management (IJSEM)
Vol 3, Issue 3, March 2018

and initial dye concentration was also studied. The adsorbent data was analyzed by isotherm and kinetic models. α-Fe2O3 acted as good adsorbent for the removal of AR 97 from its aqueous solution

II. EXPERIMENTAL DETAILS

A. Preparation and Characterization of α-Fe_2O_3 Nanopowder

The preparation of α-Fe_2O_3 nanopowder involved the use of ferric nitrate, $Fe(NO_3)_3.9H_2O$ as oxidizer and oxalyldihydrazide (ODH), $C_2H_6N_4O_2$ as fuel. Ferric nitrate was taken in a crystallizing dish of approximately 300 mL capacity and dissolved in minimum amount of double distilled water followed by the addition of appropriate amount of ODH. The mixture was stirred magnetically for about 10 minutes and the crystallizing dish was placed on a hot plate to remove the excess water. It was then introduced into a muffle furnace maintained at around 350°C. The reaction mixture first dehydrated, ignited at one spot and then burnt to yield the nanopowder. The combustion was completed in few minutes. The formation of the nanopowder can be represented by Equation 1[15].

$$2Fe(NO_3)_3(aq) + 3C_2H_6N_4O_2(s) \longrightarrow Fe_2O_3(s) + 6CO_2(g) + 9N_2(g) + 9H_2O(g) \quad (1)$$

The PXRD pattern of the nanopowder was recorded with the help of a Philips X-ray diffractometer (PW/1050/70/76) using Cu K_α radiation (λ = 1.542A°) at 30 kV and 20 mA with Ni filter. Scherer's formula (Equation 2) was used to calculate the mean crystallite size of the nanopowder[16].

$$D = \frac{k\lambda}{\beta\cos\theta} \quad (2)$$

where D is the mean crystallite size, k is a constant, λ is the wavelength of the X-rays used, β is the full width at half maximum (FWHM) and θ is the Bragg's angle. The FTIR spectrum of the nanopowder was recorded with the help of the Nicollet IMPACT 400 D FTIR spectrometer from 300 to 4000 cm^{-1} with KBr as the reference sample. The SEM micrograph of the nanopowder was recorded by using the JEOL (JSM-840A) scanning electron microscope.

B. Adsorption of Acid Red 97 by the Nanopowder

AR 97 is an anionic azo dye with molecular formula $C_{32}H_{20}N_4O_8S_2Na_2$ and molecular mass equal to 698.66 $gmol^{-1}$. Chemically, it is 1,1'-Biphenyl]-2,2'-disulfonicacid, 4,4'-bis[(2-hydroxy-naphthalenyl)azo]-disodiumsalt. It is readily soluble in water and exhibits hazardous and carcinogenic effects. Fig. 1 and 2 represent the structure and absorption spectrum of AR 97 respectively. The maximum absorbance was observed at 512 nm.

Three different initial concentrations of AR 97 viz., 20, 40 and 60 ppm were used in the batch adsorption experiments. Double distilled water was used throughout the experiments. The batch adsorption experiments were performed at room temperature. 50 mL of the dye solution was taken in a 500 mL beaker and appropriate amount of the nanopowder was added to it. The mixture was stirred magnetically in the dark for 30 minutes, centrifuged at 3000 rpm for 10 minutes using the Kemi C8C centrifuge and then the UV-visible spectrum of the supernatant was recorded between 350 and 700 nm using the ELICO SL - 159 spectrophotometer. The dosage of the adsorbent was varied from 0.1 to 1.4 gL^{-1} of the dye solution. The percentage dye removal was calculated using Equation 3 [17].

$$\%\ dye\ removal = \frac{C_o - C_e}{C_o}\ x\ 100 \quad (3)$$

where C_o and C_e are the initial and equilibrium concentrations of the dye solution.

The optimum adsorbent dosage was determined from the plot of C_e/C_0 versus the amount of the nanopowder. The optimum contact time was determined as follows. 100 mL of the dye solution was taken in the 500 mL beaker, optimum amount of the adsorbent was added to it and the mixture was stirred magnetically in the dark. A small aliquot of the mixture was taken out after every 5 minutes, centrifuged and the UV-visible spectrum of the supernatant was recorded as described earlier. The optimum contact time was determined from the C_e/C_0 versus the contact time. The experiments were performed for all the three initial concentrations of the dye solution.

The amount of dye adsorbed on the nanopowder (q) was calculated by using Equation 4 [18].

$$q = \frac{C_o - C_e}{m}\ x\ V \quad (4)$$

where V is the volume of the solution (L) and m is the mass of the adsorbent (g).

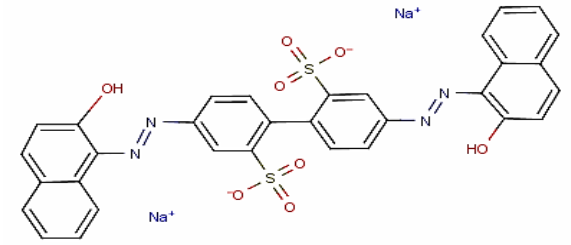

Fig. 1 Structure of Acid Red 97 dye

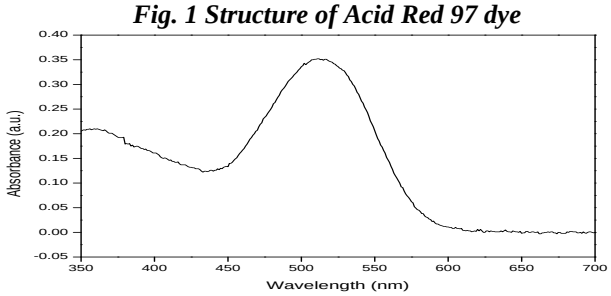

Fig. 2 Absorption spectrum of Acid Red 97 dye

ISSN (Online) 2456 -1304

International Journal of Science, Engineering and Management (IJSEM)
Vol 3, Issue 3, March 2018

III. RESULTS AND DISCUSSION

A. Characterization Results

The PXRD pattern of the nanopowder is depicted in Fig. 3. The peaks in the PXRD pattern were attributed to the hexagonal phase of α-Fe_2O_3 with JCPDS file number: 84–0311 [19]. The PXRD pattern indicated high degree of crystallinity with no impurity peaks. The mean crystallite size was found to be 25 nm. Fig. 4 illustrates the FTIR spectrum of the nanopowder. The peaks around 416 and 542 cm^{-1} were attributed to the stretching vibrations of the Fe-O bond. The peak at around 3400 cm^{-1} was assigned to the –OH group of water adsorbed on the surface of the nanopowder [20]. The SEM micrograph of the nanopowder (Fig. 5) indicated that the particles were highly agglomerated with a number of voids. The heat liberated during the combustion process is a vital factor in controlling the crystal growth. The agglomeration of the particles is usually considered as a common way of by which the nanoparticles minimize their free energy. Further, the liberation of gases during the combustion process resulted in the formation of voids [21].

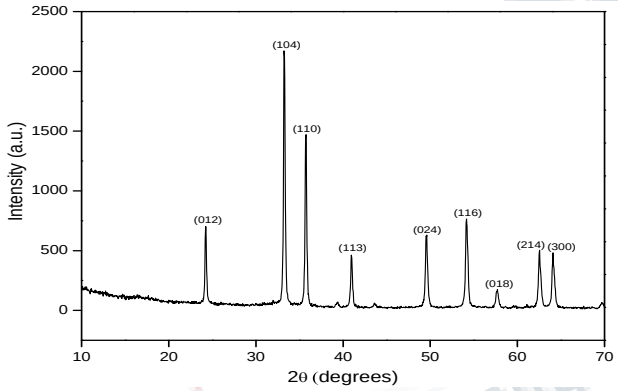

Fig. 3 PXRD pattern of the nanopowder

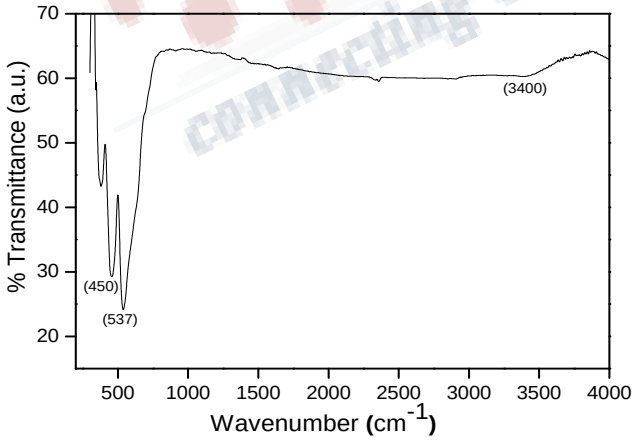

Fig. 4 FTIR spectrum of the nanopowder

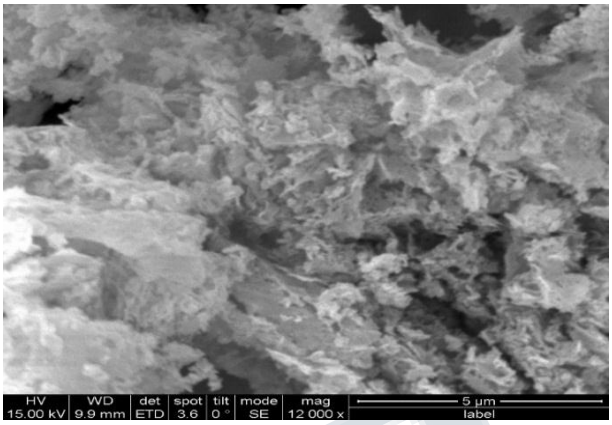

Fig. 5 SEM micrograph of the nanopowder

B. Adsorption Results

Fig. 6 depicts the effect of adsorbent dosage on the adsorption of AR 97 by the nanopowder. The adsorption increased with adsorbent dosage upto an optimum value and thereafter remained almost constant. This is because increase in adsorption increased the number of active sites available for adsorption of the dye molecules. Beyond the optimum dosage, there was negligible increase in adsorption due to the attainment of adsorption-desorption equilibrium. The optimum adsorbent dosage was found to be 0.9gL^{-1}. The effect of contact on the rate of adsorption is illustrated in Fig. 7. The adsorption increased with increase in contact time upto the optimum value and then remained almost constant. The optimum contact time was found to be 35 minutes. Table 1 describes the summary of the results for the adsorption of AR 97 by the nanopowder.

Table 1 Summary of results for the adsorption of AR 97 by the nanopowder

Initial dye concentration (ppm)	Optimum adsorbent dosage (gL^{-1})	Optimum contact time (min)	% dye removal
20	0.9	35	76.39
40	0.9	35	64.54
60	0.9	35	59.53

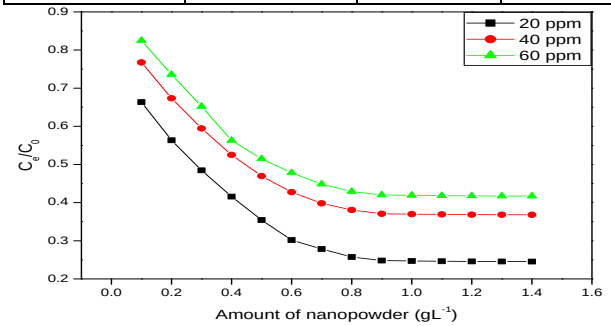

Fig. 6 Effect of adsorbent dosage on the adsorption of AR 97by the nanopowder

ISSN (Online) 2456 -1304

International Journal of Science, Engineering and Management (IJSEM)
Vol 3, Issue 3, March 2018

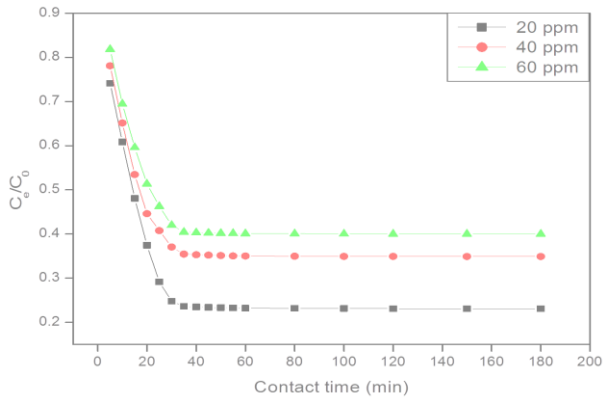

Fig. 7 Effect of contact time on the adsorption of AR 97 by the nanopowder

C. Adsorption Isotherms

The adsorption data was analysed by applying four adsorption isotherm: Langmuir, Freundlich, Dubinin-Radushkevich (D – R) and Temkin. Table 2 illustrates the linear forms of these adsorption isotherms. The adsorption obeyed Dubinin-Radushkevich and Temkin adsorption isotherms (Table 3) as depicted in Fig. 8 and 9. The values of adsorption energy (E) were more than 16 $kJmol^{-1}$ which indicated that adsorption was chemical in nature. Hence it was concluded that there were interactions between the adsorbent and the adsorbate molecules [22-25].

Table 2 Linear forms of the four adsorption isotherms

Adsorption isotherm	Linear form	Slope	Intercept
Langmuir	$\frac{C_e}{q_e} = \frac{1}{Q_0 b} + \frac{1}{Q_0} C_e$	$\frac{1}{Q_0}$	$\frac{1}{Q_0 b}$
Freundlich	$lnq_e = lnK_F + \frac{1}{n} lnC_e$	$\frac{1}{n}$	lnK_F
D - R	$lnq_e = lnQ_0 - K_{DR}\,\varepsilon^2$	$-K_{DR}$	lnQ_0
Temkin	$q_e = B_T lnK_T + B_T lnC_e$	B_T	$B_T lnK_T$

Table 3 Dubinin -Radushkevich and Temkin isotherm parameters for the removal of AR 97 by the nanopowder

Adsorption isotherm	Parameter	20 ppm	40 ppm	60 ppm
Dubinin - Radushkevich	Q_0 (mgg^{-1})	1.64	2.14	2.36
	K_{DR}	-3.16E(-6)	-2.64E(-6)	-6.89E(-5)
	E ($kJmol^{-1}$)	397.62	137.39	85.15
	R^2	0.9075	0.91	0.89
Temkin	B_T ($kJmol^{-1}$)	2.1119	4.01	4.76
	K_T (Lg^{-1})	0.5730	0.35	0.28
	R^2	0.9010	0.93	0.93

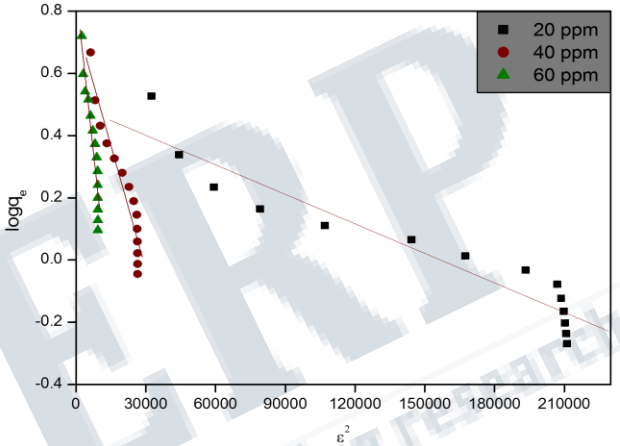

Fig. 8 Dubinin-Radushkevich adsorption isotherm

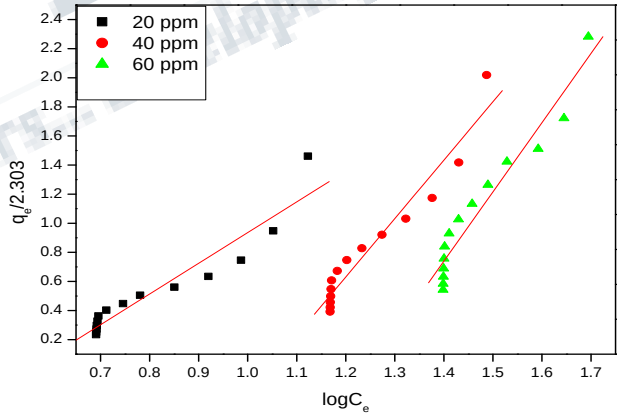

Fig. 9 Temkin adsorption isotherm

3.4. Adsorption Kinetics

Adsorption kinetic models were applied to the adsorption data to find the rate determining step in the process. Four kinetic models: the pseudo-first order, the pseudo-second order, the intraparticle diffusion (IPD) and the Elovich models were used. Table 4 represents the linear forms of the four kinetic models. As depicted in Fig. 10 the pseudo-first order model provided the best fit for the process (Table 5). The adsorption was assumed to occur in two steps; a fast first step and a slo second step [26-29].

ISSN (Online) 2456 -1304

International Journal of Science, Engineering and Management (IJSEM)
Vol 3, Issue 3, March 2018

Table 4 Linear forms of the four kinetic models

Kinetic model	Linear form	Slope	Intercept
Pseudo-first order	$\log(q_e - q_t) = \frac{-k_1 t}{2.303} + log q_e$	$\frac{-k_1}{2.303}$	$log q_e$
Pseudo-second order	$\frac{t}{q_t} = \frac{1}{k_2 q_e^2} + \frac{1}{q_e t}$	$\frac{1}{q_e}$	$\frac{1}{k_2 q_e^2}$
IPD	$q_t = k_{id}\sqrt{t} + C$	k_{id}	C
Elovich	$q_t = \beta \ln(\alpha\beta) + \beta lnt$	B_T	$B_T lnK_T$

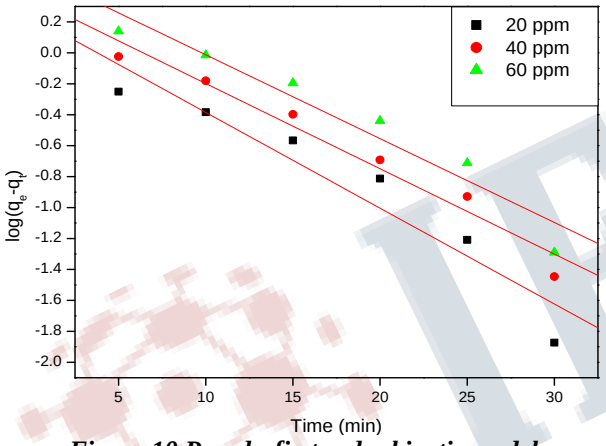

Figure 10 Pseudo-first order kinetic model

Table 5 Pseudo-firsrt order kinetic results for the adsorption of AR 97 by the nanopowder

Parameter	20 ppm	40 ppm	60 ppm
K_1 (min^{-1})	0.1426	0.1269	0.1248
R^2	0.9143	0.9636	0.9377

IV. CONCLUSION

α-Fe_2O_3 nanopowder was successfully synthesized by solution combustion method. The nanopowder was used as adsorbent for the removal of Acid Red 97 from its aqueous solution. The nanopowder acted as an effective adsorbent for the removal of the dye. It can be used as adsorbent for effective removal of other azo dyes from textile mill, paper mill and other industrial effluents.

V. ACKNOWLEDGMENTS

The authors are thankful to the TEQIP Laboratory of M.S. Ramaiah Institute of Technology for providing facilities to carry out the experimental work. MNZA is thankful to Dr. Sanaulla P.F, Head, Department of Chemistry; and Dr. Syed Abu Sayeed Mohammed, HKBK College of Engineering, Bangalore, India for useful suggestions on adsorption isotherm and adsorption kinetics.

REFERENCES

[1] M.M. Hassan, M.Z. Alam, and M.N. Anwar, "Biodegradation of textile azo dyes by bacteria isolated from dyeing industry effluent", International Research Journal of Biological Sciences, vol. 2, no. 8, pp. 27-31, August 2013.

[2] N. Daneshvar, S. Aber, and F. Hosseinzadeh, "Study of C.I. Acid Orange 7 removal in contaminated water by photo oxidation processes", Global NEST Journal, vol. 10, no. 1, pp. 16-23, 2008.

[3] M.H. Khedr, K.S. Abdel Halim, and N.K. Soliman, "Synthesis and photocatalytic activity of nano-sized iron oxides", Materials Letters vol. 63, pp. 598-601, 2009.

[4] Sushmita Banerjee and M.C. Chattopadhyaya, "Adsorption characteristics for the removal of a toxic dye, tartrazine from aqueous solutions", Arabian Journal of Chemistry, vol. 10, pp. S1629-S1638, 2017

.

[5] A.R. Rahmani, M. Zarrabi, M.R. Samarghandi, A. Afkhami, and H. R. Ghaffari, "Degradation of azo dye Reactive Black 5 and Acid Orange 7 by Fenton-like mechanism", Iranian Journal of Chemical Engineering, vol. 7, no. 1, pp. 87-94, Winter 2010.

[6] R.S. Raveendra, P.A. Prashanth, R. Hari Krishna, N.P. Bhagya, B.M. Nagabhushana, H. Raja Naika, K. Lingaraju, H. Nagabhushana, and B. Daruka Prasad, "Synthesis, structural characterization of nano $ZnTiO_3$ ceramic: An effective azo dye adsorbent and antibacterial agent", Journal of Asian Ceramic Societies, vol. 2, pp. 357–365, 2014.

[7] A.R. Khataee, M. Safarpour, A. Naseri, and M. Zarei, "Photoelectro-Fenton/nanophotocatalysis decolorization of three textile dyes mixture: Response surface modeling and multivariate calibration procedure for simultaneous

determination", Journal of Electroanalytical Chemistry, vol. 672, 53–62, 2012.

[8] Rajesh Kumar, S. Gautam, In-Chul Hwang, Jae Rhung Lee, K.H. Chae, and Nagesh Thakur, "Preparation and characterization of α-Fe_2O_3 polyhedral nanocrystals via annealing technique", Materials Letters, vol. 63, pp. 1047-1050, 2009.

[9] Wei Zheng, Zhenyu Li, Hongnan Zhang, Wei Wang, Yu Wang, and Ce Wang, "Electrospinning route for α-Fe_2O_3 ceramic nanofibers and their gas sensing properties", vol. 44, no. 6, pp. 1432-1436, June 2009.

[10] Wei Jin, Baitao Dong, Wen Chen, Chunxia Zhao, Liqiang Mai, and Ying Dai, "Synthesis and gas sensing properties of Fe_2O_3 nanoparticles activated V_2O_5 nanotubes", Sensors and Actuators B, vol. 145, 211-215, 2010.

[11] Prita P. Sarangi, Bhanudas Naik, and N.N. Ghosh, Low temperature synthesis of single-phase α-Fe_2O_3 nano-powders by using simple but novel chemical methods", Powder Technology, vol. 192, no. 3, pp. 245-249, 2009.

[12] Jiao Hua, and Yang Heqing, "Thermal decomposition synthesis of 3D urchin- like α-Fe2O3 Superstructures", Materials Science and Engineering B, vol. 156, pp. 68-72, 2009.

[13] Slavica Stankic, Sneha Suman, Francia Haque, and Jasmina Vidic, "Pure and multi metal oxide nanoparticles: synthesis, antibacterial and cytotoxic properties", Journal of Nanobiotechnology, vol. 14, pp. 73-92, 2016.

[14] , Paul Epstein and Peter Dinka, "Solution combustion synthesis of nanomaterials, Proceedings of the Combustion Institute", vol. 31, no. 2, pp. 1789-1795, January 2007.

[15] M.N. Zulfiqar Ahmed, K. B. Chandrasekhar, A. A. Jahagirdar, H. Nagabhushana, and B. M. Nagabhushana, "Photocatalytic activity of nanocrystalline ZnO, α-Fe_2O_3 and $ZnFe_2O_4$/ZnO", Applied Nanoscience, vol. 5, pp. 961–968, 2015.

[16] Ritu Rani, Gagan Kumar, Khalid Mujasam Batoo, and M. Singh, "Electric and dielectric study of zinc substituted cobalt nanoferrites prepared by solution combustion method", American Journal of Nanomaterials, vol. 1, no. 1, pp. 9-12, 2013.

[17] Miaoliang Huang, Chunfang Zibao Wu, Yunfang Huang, Jianming Lin, and Jihuai Wu, "Photocatalytic discolorization of methyl orange solution by Pt modified TiO_2 loaded on natural zeolite", Dyes and Pigments, vol. 77, pp. 327-334, 2008.

[18] D.A. Fungaro, M. Yamaura, and T.E.M. Carvalho, "Adsorption of anionic dyes from aqueous solution on zeolite from fly ash-iron oxide magnetic nanocomposite", Journal of Atomic and Molecular Sciences, vol. 2, no. 4, pp. 305-316, 2011.

[19] T.P. Raming, A.J.A. Winnubst, C.M. Kats, and P.A. Philips, "The synthesis and magnetic properties of nanosized hematite (α-Fe_2O_3) particles", Journal of Colloid and Interface Science, vol. 249, pp. 346-350, 2002.

[20] A.A Jahagirdar, M.N. Zulfiqar Ahmed, N. Donappa. H. Nagabhushana, and B. M. Nagabhushana,"Synthesis, characterization and dye degradation activity of α-Fe_2O_3", IJETA-ETS, vol. 5, pp. 144-147, 2011.

[21] N. Dhananjaya, H. Nagabhushana, B.M. Nagabhushana, B. Rudraswamy, C. Shivakumara, and R.P.S. Chakradhar, "Effect of Li^+ ion on enhancement of photoluminescence in Gd_2O_3: Eu^{3+} nanophosphors prepared by combustion technique",Journal of Alloys and Compounds, vol. 509, no. 5, pp. 2368- 2374, February 2011.

[22] J.S. Piccin, G.L. Dotto and L.A.A. Pinto, "Adsorption isotherms and thermochemical data of fd&c red n° 40 binding by chitosan", Brazilian Journal of Chemical Engineering", vol. 28, no. 2, pp. 295-304, 2011.

[23]. Xunjun Chen, "Modeling of Experimental Adsorption Isotherm Data", Information, vol. 6, 14-22, 2015.

[24] A.U. Itodo and H.U. Itodo, "Sorption energies estimation using Dubinin-Radushkevich and Temkin adsorption isotherms", Life Science Journal, vol. 7, no. 4, pp. 31-39, 2010.

[25] S.A. Umoren, U.J. Etim, and A.U. Israel, "Adsorption of methylene blue from industrial effluent using poly(vinyl alcohol)", Journal of Materials and Environmental Science, vol. 4, no. 1, pp. 75-86, 2013.

[26] P. Senthil Kumar, and K. Kirthika, "Equilibrium and kinetic study of adsorption of nickel from aqueous solution onto bael tree leaf powder", Journal of Engineering Science and Technology, vol. 4, no. 4, pp. 351-363, 2009.

[27] J. Malina, and A. Rađenović, "Kinetic aspects of methylene blue adsorption on blast furnace sludge", Chemical and Biochemical Engineering Q., vol. 28, no. 4, pp. 491-498, 2014.

[28] Ch. Sekhararao Gulipalli, B. Prasad, and Kailas L. Wasewar, "Batch study, equilibrium and kinetics of adsorption of selenium using rice husk ash (RHA)", Journal of Engineering Science and Technology, vol. 6, no. 5, pp. 586-605, 2011.

[29] M. Can, "Studies of the kinetics for rhodium adsorption onto gallic acid derived polymer: the application of nonlinear regression analysis, Acta Physica Polonica A, vol. 127, pp. 1308-1310, 2015